Scientific Papers of
the Institute of Electrical Power Engineering of
the Wrocław University of Technology

PRESENT PROBLEMS OF POWER SYSTEM CONTROL

4

Wrocław 2013

Printed in the camera ready form

Institute of Electrical Power Engineering
Wrocław University of Technology
Wybrzeże Wyspiańskiego 27, 50-370 Wrocław, Poland
phone: +48 71 320 26 55, fax: +48 71 320 26 56
www: http://www.ie.pwr.wroc.pl/; e-mail: Inst.Energ@pwr.wroc.pl

OFICYNA WYDAWNICZA POLITECHNIKI WROCŁAWSKIEJ
Wybrzeże Wyspiańskiego 27, 50-370 Wrocław
http://www.oficyna.pwr.wroc.pl
e-mail: oficwyd@pwr.wroc.pl
zamawianie.ksiazek@pwr.wroc.pl

ISSN 2084-2201

Drukarnia Oficyny Wydawniczej Politechniki Wrocławskiej. Order No. 706/2013.

arc fault, fault location,
signal processing, filtration

Mateusz PUSTUŁKA*, Jan IŻYKOWSKI*,
Mirosław ŁUKOWICZ*

NEURAL NETWORK FILTRATION FOR ARC FAULTS LOCATION ON POWER TRANSMISSION LINES

This paper presents filtration using neural network for arc fault location, which allows to determine the distance to a fault, as a result of considering natural fault loops. It is assumed that three-phase voltages and currents from both ends of the line are the input signals of the fault locator and naturally of the neutral network applied for filtering the input signals. In addition to natural fault loop signals also use of symmetrical components (positive and negative or incremental positive sequence components) to fault location were considered as well. Results of evaluation study have been included, analyzed and discussed. Influence of filtration has been also considered.

1. INTRODUCTION

The reliable operation of the electric power grid is one of the main goals of power system operators. Reduction of the duration of outages is one of the key requirements. There are many different ways that this goal can be achieved, with accurate fault location for an inspection-repair purpose [2, 5, 6] being one of them.

Algorithms for accurate location of faults on power lines have been a subject of great interest of researchers since the power system reliability became an important factor for network operators and customers [6]. Among the known methods, the approach based on an impedance principle is the most popular and most frequently implemented into protective relays or stand alone fault locators (FL). In particular, the algorithms utilizing one-end current and voltage measurements have been

* Institute of Electrical Power Engineering, Wroclaw University of Technology, Wroclaw, Poland.

introduced at the beginning. Then two-end fault location principle [5, 6] has been extensively explored. This principle is considered in this paper.

Neural networks are one of the fastest growing artificial intelligence techniques. Due to the ability to learn and adapt they have a high potential. Series of patterns based on heuristic knowledge are presented to neural network in the learning process. Artificial neural network acquires the ability to appropriately respond included in the learning database.

The main task for neural network applied in this study will be prediction of steady state signals obtained by using current and voltage signals from the interval just after fault inception. The computer models of transmission system developed for this purpose were used for generating large number of short-circuit cases. The variability ranges of the system parameters was adopted for modeling faults. Either fault location, fault resistance and short-circuit power of equivalent sources behind line terminals were changed in random. Size of population generated for neural network learning process was 1000 cases and for testing it was 100 cases. Results of evaluation study have been included and discussed.

Fault location algorithm was performed using the signals generated by simulating arc faults on the transmission line: 400 kV (Fig. 1), 50 km with the aid of ATP-EMTP software [1]. The representative results for the single-phase arc fault: L1-E are presented further. Current and voltage measurements were carried out at both ends of the line.

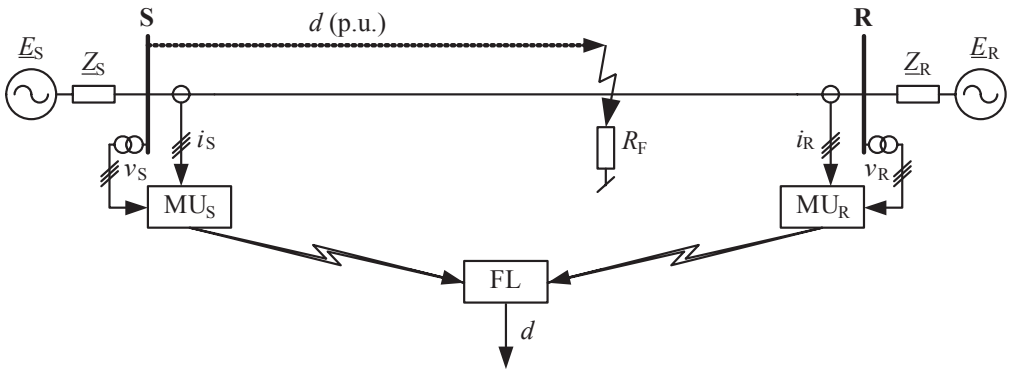

Fig. 1. Schematic diagram of two-end fault location

2. ARC FAULTS

The main aim of this study is to develop a neural network filtration for arc fault locator, therefore suitable arc fault model had to be introduced to the system model. Dynamic arc model was adopted in the form of the differential equation [3]

$$\frac{dg_p}{dt} = \frac{1}{T_p}\left(G_p - g_p\right) \tag{1}$$

where:

g_p – dynamic arc conductance,

G_p – stationary arc conductance,

T_p – time constant.

Using the ATP–EMTP program [1] for arc fault simulation, the arc can be reflected with the non-linear resistor – defined in the ELECTRICAL NETWORK unit, while the arc model – in the MODELS (Fig. 2). The arc current (Fig. 3a, b) as the input quantity is measured on-line and the non-linear differential equation (1) is being

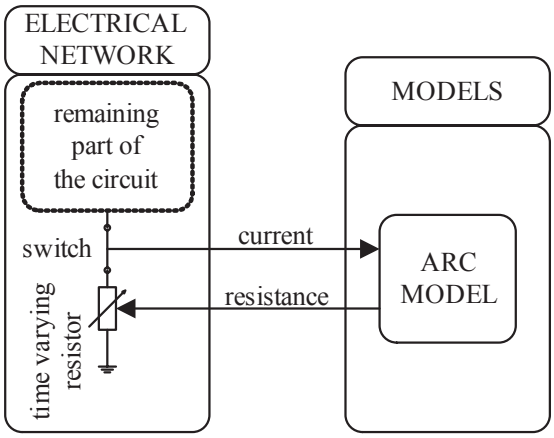

Fig. 2. Modeling arc with ATP–EMTP

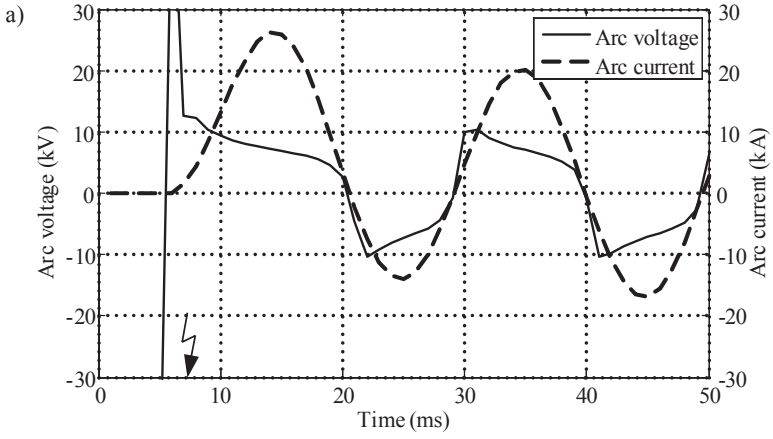

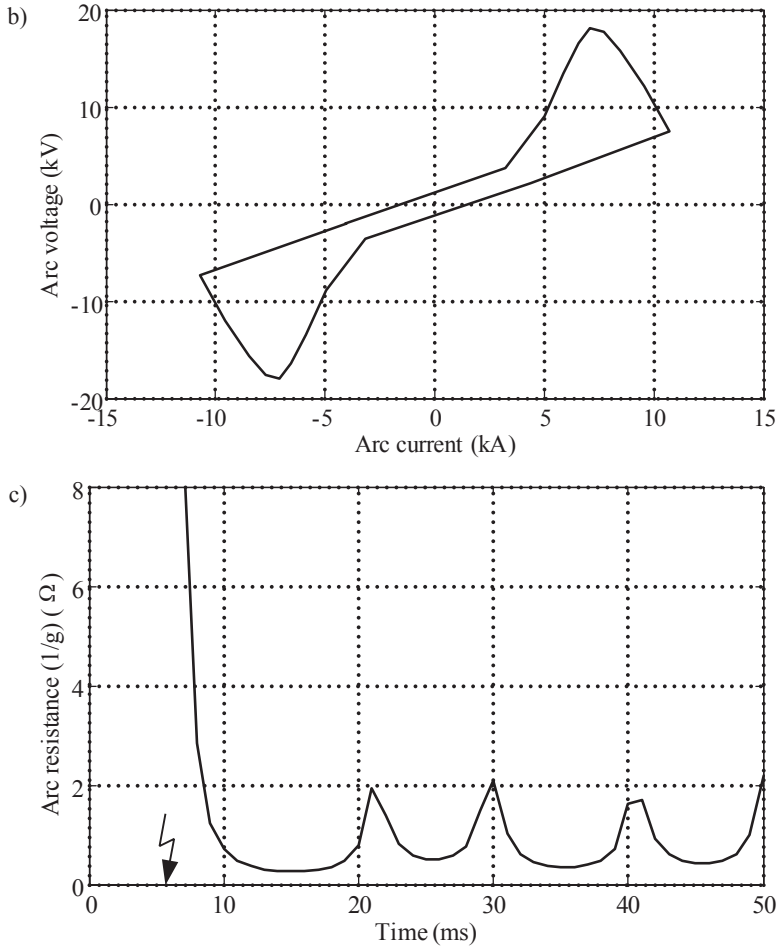

Fig. 3. Modeling of arc: a) arc current and voltage,
b) arc voltage vs. arc current (for single cycle), c) arc resistance

solved. As a result, the arc resistance is determined and transferred for fixing the resistor modeling the arc.

The model (1) allows the arc conductance $g(t)$ to be determined, from which the arc resistance is calculated (Fig. 3c).

3. FAULT LOCATION ALGORITHM

Natural fault loops, identical as for a distance protection, are considered [4, 5]. For this purpose, the relaying signals (both voltage and current fault loop signals) are

formed accordingly to the fault type. Table 1 defines those signals to any consideration of fault loops seen from the S end of the line for a single-circuit line (Fig. 4). Signals for fault loop seen from the R end are composed analogously.

In a case of phase-to-earth fault the voltage and current of a given faulted phase are taken, but the component associated with the zero-sequence component: zero-sequence current ($\underline{I}_{S0}$) multiplied by the factor: $k_0 = (\underline{Z}_{0L} - \underline{Z}_{1L})/\underline{Z}_{1L}$ is added to the phase current. This results from the fact that the impedances of the line for the positive sequence ($\underline{Z}_{1L}$) and zero sequence ($\underline{Z}_{0L}$) are not identical, and the impedance of the line section between the measuring point (S) and the fault point (F) for the positive sequence ($d\underline{Z}_{1L}$) is a measure of the distance to fault (d (p.u.)) – Fig. 4.

For a fault loop phase 1-to-phase 2, the differences of voltages and currents from the phases involved in the fault, respectively, are taken as the fault loop signals. As a result of the subtraction, the zero sequence component is eliminated and there is no compensation due to different line impedances for the positive and zero sequences.

Figure 4 shows the models of the considered fault loops (Fig. 4a, b) and the aggregated model (Fig. 4c).

Table 1. Composition of fault loop voltage and current signals for single-circuit line

Fault type	Fault loop voltage	Fault loop current
L1–E	$\underline{V}_{S\_L1}$	$\underline{I}_{S\_L1} + \underline{k}_0 \underline{I}_{S0}$
L2–E	$\underline{V}_{S\_L2}$	$\underline{I}_{S\_L2} + \underline{k}_0 \underline{I}_{S0}$
L3–E	$\underline{V}_{S\_L3}$	$\underline{I}_{S\_L3} + \underline{k}_0 \underline{I}_{S0}$
L1–L2, L1–L2–E, (L1–L2–L3, L1–L2–L3–E)*	$\underline{V}_{S\_L1} - \underline{V}_{S\_L2}$	$\underline{I}_{S\_L1} - \underline{I}_{S\_L2}$
L2–L3, L2–L3–E	$\underline{V}_{S\_L2} - \underline{V}_{S\_L3}$	$\underline{I}_{S\_L2} - \underline{I}_{S\_L3}$
L3–L1, L3–L1–E	$\underline{V}_{S\_L3} - \underline{V}_{S\_L1}$	$\underline{I}_{S\_L3} - \underline{I}_{S\_L1}$
* – includes loop L1–L2, but also loops L2–L3, L3–L1 can be analyzed, $\underline{k}_0 = \dfrac{\underline{Z}_{0L} - \underline{Z}_{1L}}{\underline{Z}_{1L}}$.		

Fault loop seen from the S end (Fig. 4a) consists of a line section of the positive sequence impedance: $d\underline{Z}_{1L}$ and the transverse branch that represents a fault (resistance: R_{arc}). In case of the fault loop seen from the R end (Fig. 4b) impedance of the line section for the positive sequence is: $(1 - d)\underline{Z}_{1L}$ and the transverse branch is as in the previous fault loop (Fig. 4a).

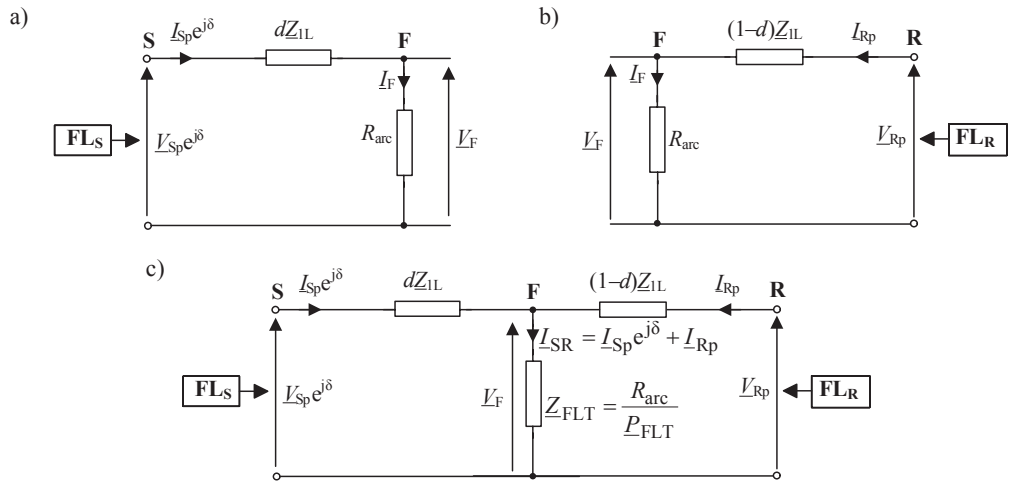

Fig. 4. Models of fault loop measurement for:
a) relay at bus S, b) relay at bus R, c) aggregated model

Use of unsynchronized measurements from both ends of the line is considered and the measurements from the R end (fault loop voltage and current: $\underline{V}_{Rp}$, $\underline{I}_{Rp}$) are assumed as a reference base. Therefore, the measurements from the S end (fault loop voltage and current: $\underline{V}_{Sp}$, $\underline{I}_{Sp}$) are synchronized analytically with use of the synchronization operator: $e^{j\delta}$, where δ – unknown synchronization angle. This is achieved by multiplying the phasors of the original fault loop signals of the bus S by this operator. In case of the availability of synchronized measurements the elements associated with the determination of the synchronization angle should be omitted.

Aggregating both fault loop models from Fig. 4a and b leads to the model as shown in Fig. 4c. There is a fictitious transverse branch, through which flows the total current ($\underline{I}_{Sp}\, e^{j\delta} + \underline{I}_{Rp}$) and not, as in reality: $\underline{I}_F$. Therefore, to provide the voltage in this branch: $\underline{V}_F$, as it is present in reality, the impedance of this fictitious branch ($\underline{Z}_{FLT}$) is not equal to the fault path resistance (R_{arc}). This impedance ($\underline{Z}_{FLT}$) matches the arc resistance (R_{arc}) divided by the complex factor: $\underline{P}_{FLT}$, which depends on the type of a fault (Table 2) [5].

Table 2. Coefficient $\underline{P}_{FLT}$ for different fault types

Fault type	$\underline{P}_{FLT}$
L1–E, L2–E, L3–E	$\frac{2\underline{Z}_{1L} + \underline{Z}_{0L}}{3\underline{Z}_{1L}}$
L1–L2, L2–L3, L3–L1	2
L1–L2–E, L2–L3–E, L3–L1–E, L1–L2–L3, L1–L2–L3–E	1

Comparison of voltage on the transverse branch, i.e. at the fault point (F) – determined from the S and R line ends (Fig. 4), respectively, yields:

$$\underline{V}_{\mathrm{Sp}}\mathrm{e}^{j\delta} - d\,\underline{Z}_{1\mathrm{L}}\,\underline{I}_{\mathrm{Sp}}\mathrm{e}^{j\delta} = \underline{V}_{\mathrm{Rp}} - (1-d)\underline{Z}_{1\mathrm{L}}\,\underline{I}_{\mathrm{Rp}} \tag{2}$$

Equation (2) can be written separately for the real and imaginary parts. This gives a system of two equations with two unknowns: d – fault distance (p.u.), δ – synchronization angle. It can be solved using very well-known numerical procedures. However, one may face problems with obtaining a valid solution. In fact, the unknowns are: d, $\sin(\delta)$, $\cos(\delta)$ while the synchronization angle δ can be positive or negative, i.e. in the following range: $-\pi <= \delta <= \pi$. Only one solution, out of two, is a valid one.

In order to avoid iterative calculations it is proposed to specify the modulus (absolute value) for the synchronization operator $\mathrm{e}^{j\delta}$ determined from (2) as follow:

$$\left|\mathrm{e}^{j\delta}\right| = \left|\frac{\underline{V}_{\mathrm{Rp}} - \underline{Z}_{1\mathrm{L}}\,\underline{I}_{\mathrm{Rp}} + d\,\underline{Z}_{1\mathrm{L}}\,\underline{I}_{\mathrm{Rp}}}{\underline{V}_{\mathrm{Sp}} - d\,\underline{Z}_{1\mathrm{L}}\,\underline{I}_{\mathrm{Sp}}}\right| \tag{3}$$

This gives:

$$\left|\underline{V}_{\mathrm{Rp}} - \underline{Z}_{1\mathrm{L}}\,\underline{I}_{\mathrm{Rp}} + d\,\underline{Z}_{1\mathrm{L}}\,\underline{I}_{\mathrm{Rp}}\right| = \left|\underline{V}_{\mathrm{Sp}} - d\,\underline{Z}_{1\mathrm{L}}\,\underline{I}_{\mathrm{Sp}}\right| \tag{4}$$

After tedious manipulations on (4) the following quadratic equation for the sought distance to fault is obtained:

$$A_2 d^2 + A_1 d + A_0 = 0 \tag{5}$$

where: A_2, A_1, A_0 – coefficients (real numbers) specified by the phasors of fault loop signals [4]: ($\underline{V}_{\mathrm{Sp}}$, $\underline{I}_{\mathrm{Sp}}$) and ($\underline{V}_{\mathrm{Rp}}$, $\underline{I}_{\mathrm{Rp}}$), obtained with unsynchronized measurements at both ends of the line, and by the impedance of the line for the positive sequence ($\underline{Z}_{1\mathrm{L}}$).

The solution of (5) gives two results for the sought fault distance (d_1, d_2). At least one of them indicates a detected fault in the line. If only one solution is such that it is satisfied: $0 < (d_1$ or $d_2) < 1$, then in a natural way this solution is taken as the correct (valid). On the other hand, if it is obtained that the two solutions indicate a fault in the line: $0 < (d_1$ and $d_2) < 1$, an additional selection of a solution that is correct has to be performed. Determination of the correct solution, which corresponds to the actual fault, can be determined by analyzing the estimated fault location when the input signals of the fault locator are symmetrical components of voltages and currents from both ends of the lines (Fig. 5).

As the input signals of the fault locator also symmetrical components of voltages and currents from both ends of the lines can be used: positive and negative – for asymmetrical faults, positive and incremental positive – for symmetrical three-phase faults.

In this case one needs replacing the fault loop signals in the derived equations (5) by the corresponding symmetrical components.

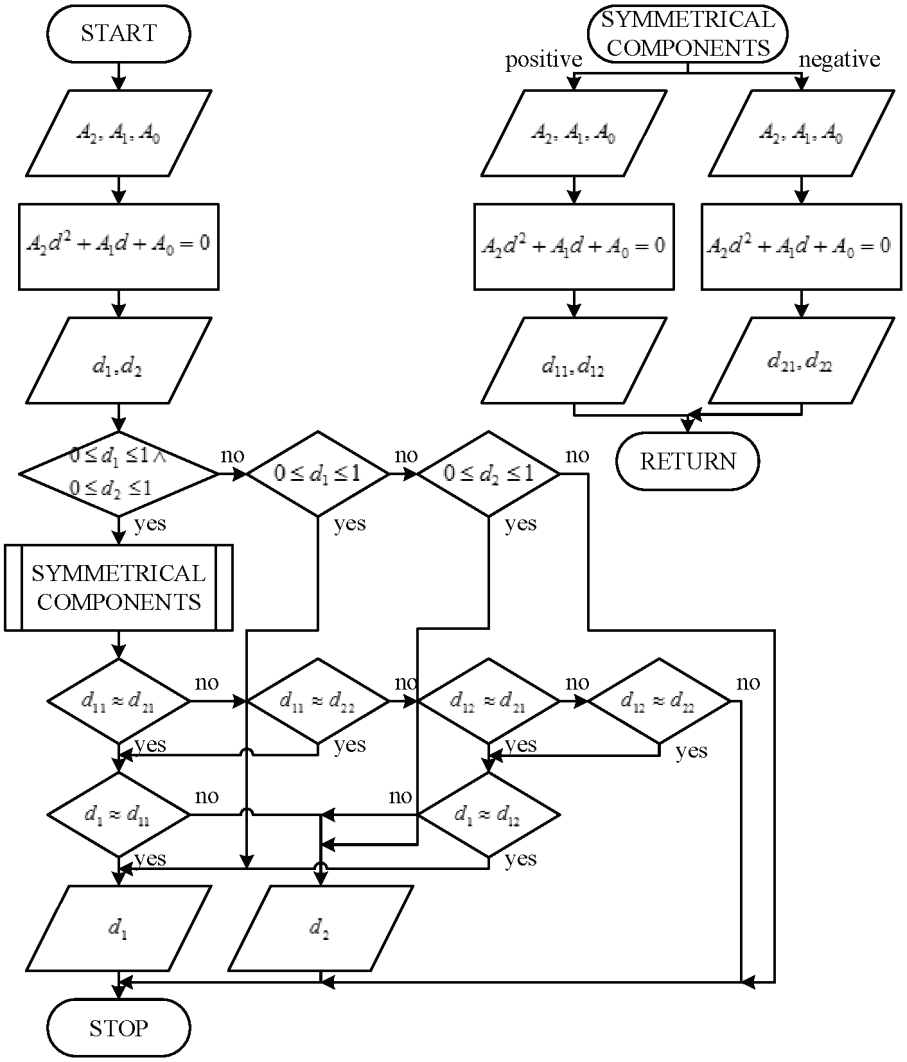

Fig. 5. The flowchart for calculating valid solution (main program with sub procedure)

4. ARTIFICIAL NEURAL NETWORK

Artificial neural network (ANN) used in the study contains two hidden layers consisting of 20 neurons and the output layer with 1 neuron (Fig. 6). Input vectors were

selected from the period 20ms just after fault (Fig. 7). A block diagram (Fig. 8) presents position of ANN in location procedure. There are used as many neural networks as many signals have to be filtrated.

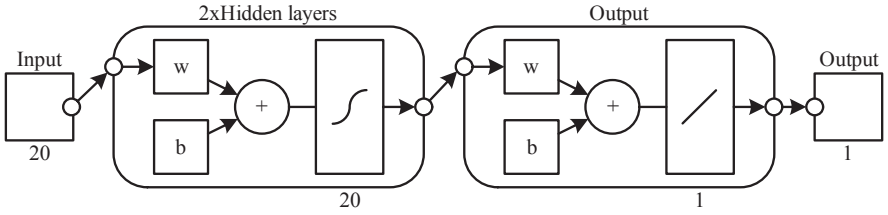

Fig. 6. Multilayer ANN

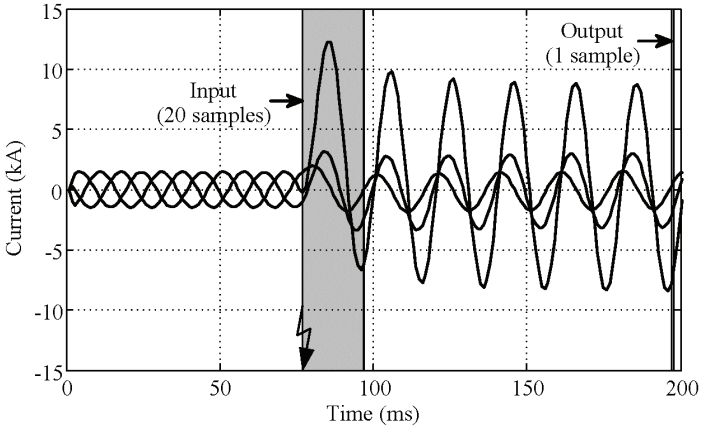

Fig. 7. Example of input and output of i_S for training ANN

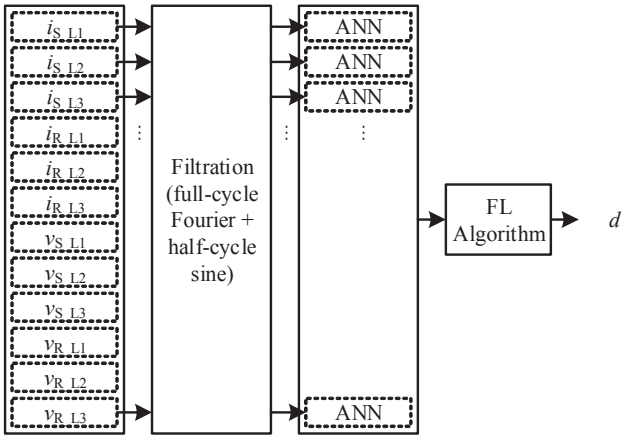

Fig. 8. The flowchart of investigated method

Before starting the learning process, inputs and outputs of the network were normalized using the scaling function so that it always belonged to the range (–1, 1) and divided into learning, testing and validation data, respectively in a ratio of 70–15–15 cases. Network output corresponds directly to the target values. Tests were performed on different data (size of the population approximately 100 cases).

5. RESULTS

In statistical evaluation of the accuracy of particular fault location method, different measures for the fault location error are determined, as maximum, average, median (which gives result more resistant to extreme values, outlier elements) and standard deviation values. It is characteristic that the absolute value is usually taken for the nominator from the definition of the fault location error formula, thus can be written as follow

$$\text{Error}(\%) = \frac{\left|d - d_{\text{exact}}\right|}{l} 100\% \tag{6}$$

where:

d, d_{exact} – estimated and exact distance to the fault (in km or in relative units: p.u.),

l – total line length (in km or in if relative units are used: $l = 1$ p.u.).

Table 3 presents solutions taken in 20ms after fault incipience for arc fault location algorithm and for arc fault location algorithm when solutions have been taken in 40ms after fault incipience. Both cases were considered with and without ANN.

Standard full-cycle Fourier filtration was used as the basic in the considered location algorithms. It has been found that in some cases, the applied such filtering alone appears as insufficient due to a severe distortion of the processed signals. It was a subject of research that performing the averaging of the results of the location in the fourth cycle after the fault, instead of averaging in the third cycle, significantly improves accuracy. Of course, this is possible only if the fault is not switched off earlier. An alternative approach to this is based on introducing an additional pre-filtering, leaving the averaging within the 3rd cycle – as was assumed at the beginning of the study. Additional pre-filtration was used with a half-cycle sine filter. It has been found that such extra pre-filtering contributes to a significant improvement of the fault location accuracy.

Selection of the valid solution (consistent with the actual fault) out of the two obtained from the quadratic equation (5) was performed as follows: the valid solution is determined by taking the solution for which there is a coincidence of the results obtained for two different components (when the input signals of the fault locator are symmetrical components of voltages and currents from both ends of the

lines), which in practice means that they are very close to each other, while for the other solution (to be rejected) there are significant differences; only one of the solutions for the fault distance indicates a fault in the line and it is naturally assumed to be the valid solution.

Table 3. Results for 10 from 100 test cases

Accurate fault distance (km)	ANN + Algorithm_t_{20} (km)	Error [%]	Algorithm_t_{20} (km)	Error [%]	Algorithm_t_{40} (km)	Error [%]	ANN + Algorithm_t_{40} (km)	Error [%]
5,00	5,11	0,22	5,14	0,28	5,06	0,13	4,93	0,14
10,00	10,32	0,64	7,57	4,86	10,10	0,20	9,99	0,03
15,00	14,84	0,31	12,49	5,03	15,33	0,65	14,82	0,36
20,00	20,54	1,09	21,14	2,28	19,72	0,56	19,98	0,04
25,00	25,02	0,05	30,00	10,00	24,57	0,86	24,87	0,27
30,00	30,45	0,89	29,05	1,89	29,93	0,15	29,82	0,36
35,00	35,19	0,37	36,70	3,40	34,91	0,19	33,06	3,88
40,00	39,17	1,67	37,47	5,06	39,78	0,43	39,57	0,87
45,00	44,86	0,29	54,86	19,71	43,91	2,18	44,93	0,14
max		1,67		19,71		2,18		3,88
average		0,61		5,83		0,59		0,68
median		0,37		4,86		0,43		0,27
std. deviation		0,52		5,89		0,65		1,23

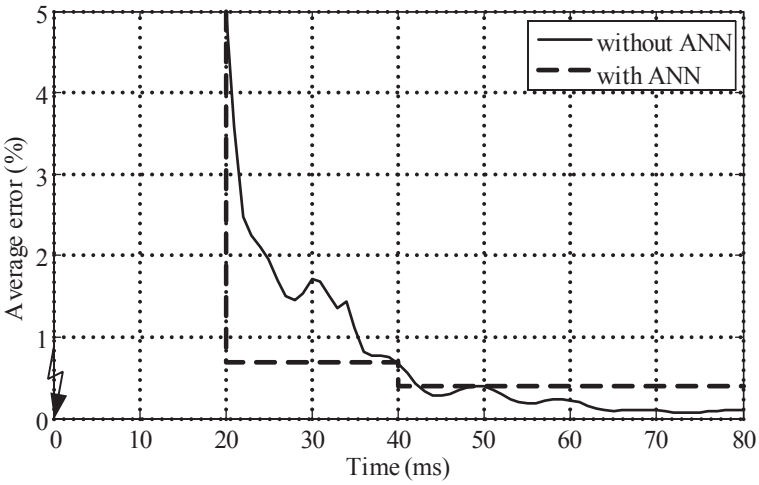

Fig. 9. Comparison of average error for algorithm with and without ANN

Better accuracy was achieved by using fault loop signals and it is slightly better than the location with using of the measured data from one end of the line. This is the effect that in case of measurements at one end only, as a result of insufficient information there is a need for introducing simplifying assumptions.

Comparison of fault location methods (with and without ANN) is shown in Fig. 9. In both cases there has been used the standard full-cycle Fourier filtering combined with the pre-filtering in the form of a half-cycle sine filter.

6. CONCLUSION

Arc fault location on transmission lines with use of voltage and current measurements from both ends of the line acquired asynchronously has been considered. The derived algorithm applies the fault loop signals from the two ends of the line as the fault locator inputs. Quadratic equation for the sought distance to fault, whose coefficients are expressed in a compact form, has been obtained. The selection of the valid solution (out of the two possible) is obtained by taking the solution for which there is a coincidence of the results obtained for two different components (when the input signals of the fault locator are symmetrical components of voltages and currents from both ends of the lines).

The derived algorithm can also be useful when symmetrical components of measured voltages and currents are applied as the only locator input signals. One should then use: positive and negative sequence components for asymmetrical faults and positive and incremental positive sequence for three-phase symmetrical faults. For a valid solution there is a coincidence of the results obtained for two different components, which in practice means that they are very close to each other, while for the other solution (to be rejected) there are significant differences. This approach was used as an assistance for calculating the valid solution.

The results of the study indicate the important role of digital filtering of the processed signals that are severely distorted under arc faults. It is reasonable to take a direct result of the calculations or results averaged – as late as possible after fault incipience, but before its elimination. It has been shown that using the standard full-cycle Fourier filtering combined with the pre-filtering in the form of a half-cycle sine filter and additional ANN improves considerably the accuracy of the calculation results. Moreover the results with lower errors are estimated in shorter time.

Analyzed application of measurements from both sides of the line to fault location does not require introducing the simplifying assumptions, which are necessary if the location is performed with only the local measurements. As a result, better accuracy is obtained. Further improvement of fault location accuracy can be achieved by taking into account the distributed-parameter line model for lines of considerable length.

Fault location algorithm with neural network filtration compared with alone algorithm gives better results. A comparative analysis has been prepared based on average error, median, maximum and standard deviation. Presented average errors of convergence show neural network as a method characterized by lower errors than algorithm which gives solution after 20ms and comparable results than algorithm with solution after 40ms.

REFERENCES

[1] DOMMEL H.W., *Electro-Magnetic Transients Program*, BPA, Portland, Oregon, 1986.
[2] FILOMENA A.D., RESENDER M., SALIM R.H., BRETAS A.S., *Fault location for underground distribution feeders: An extended impedance-based formulation with capacitive current compensation*, International Journal of Electrical Power & Energy Systems, Vol. 31, No. 9, October 2009, 489–496.
[3] JOHNS A.T., AGGARWAL R.K., SONG Y.H., *Improved techniques for modelling fault arcs an faulted EHV transmission systems*, Generation, Transmission and Distribution, IEE Proceedings, Vol. 141, No. 2, 1994, 148–154.
[4] PUSTUŁKA M., IŻYKOWSKI J., ŁUKOWICZ M., *Zastosowanie sztucznych sieci neuronowych do lokalizacji zwarć łukowych na elektroenergetycznych liniach przesyłowych*. Sieci Elektroenergetyczne w Przemyśle i Energetyce, VII Konferencja naukowo-techniczna, Szklarska Poręba, 19–21 września 2012.
[5] SAHA M.M., IŻYKOWSKI J., ROSOŁOWSKI E., *Fault Location on Power Networks*, Springer, London 2010.
[6] SAHA M.M., ROSOŁOWSKI E., IŻYKOWSKI J., *New fault location method – incorporated in current differential protective relays for series compensated transmission lines*, PACWorld, Vol. 21, September 2012, 54–59.